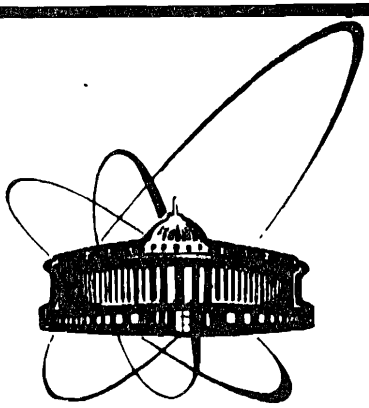

объединенный
институт
ядерных
исследований
дубна

E1-87-689

A HIGH STATISTICS MEASUREMENT OF THE PROTON STRUCTURE FUNCTION AND TESTS OF QCD FROM DEEP INELASTIC MUON SCATTERING AT HIGH Q^2

BCDMS Collaboration

Submitted the the International Europhysics
Conference on High Energy Physics,
Uppsala, June 25 - July 1, 1987

1987

A.C.Benvenuti, D.Bollini, G.Bruni, T.Camporesi, L.Monari and F.L.Navarria
Dipartimento di Fisica dell'Università and INFN, Bologna, Italy

A.Argento[1], J.Cvach[2], W.Lohmann[3], L.Piemontese[4] and P.Zavada[2]
CERN, Geneva, Switzerland

A.A.Akhundov, V.I.Genchev, I.A.Golutvin, Yu.T.Kiryushin, V.G.Krivokhizhin, V.V.Kukhtin, R.Lednicky, S.Nemecek, P.Reimer, I.A.Savin, G.I.Smirnov, J.Strachota, G.Sultanov[5], P.Todorov and A.G.Volodko
Joint Institute for Nuclear Research, Dubna

D.Jamnik[6], R.Kopp[7], U.Meyer-Berkhout, A.Staude, K.-M.Teichert, R.Tirler[8], R.Voss and C.Zupancic
Sektion Physik der Universität, München, Federal Republic of Germany[9]

J.Feltesse, A.Milsztajn, A.Ouraou, J.F.Renardy, P.Rich-Hennion, Y.Sacquin, G.Smadja and M.Virchaux
DPhPE, CEN Saclay, France

[1]Now at Digital Equipment, Torino, Italy
[2]On leave from Institute of Physics, CSAV, Prague, Czechslovakia
[3]On leave from the Institute für Hochenergiephysik der AdW der DDR, Berlin-Zeuthen, GDR
[4]Now at INFN, Trieste, Italy
[5]Now at the Institute of Nuclear Research and Nuclear Energy, Bulgarian Academy of Sciences, Sofia, Bulgaria
[6]On leave from E.Kardelj University and the J.Stefan Institure, Ljubljana, Yugoslavia
[7]Now at Siemens AG, Münich, FRG
[8]Now at DPhPE, CEN Saclay, France
[9]Funded in part by the German Federal Minister for Research and Technology (BMFT) under contract number 054MU12P6

In this paper, we present new results on the structure function of the proton measured with high precision in deep inelastic scattering of muons on a hydrogen target. In the one-proton exchange approximation, the deep inelastic muon-proton cross section can be written as

$$\frac{d^2\sigma}{dQ^2dx} = \frac{4\pi\alpha^2}{Q^4 x}\cdot\left[1 - y - \frac{Q^2}{4E^2} + \frac{y^2E^2 + Q^2}{2E^2[R(x,Q^2)+1]}\right]\cdot F_2(x,Q^2), \quad (1)$$

where E is the energy of the incident beam; Q^2, the squared four-momentum transfer between the muon and the hadronic system; and x and y are the Bjorken scaling variables. $F_2(x,Q^2)$ is the proton structure function and $R = \sigma_L/\sigma_T$ is the ratio of absorption cross sections for virtual photons of longitudinal and transverse polarization.

The data were collected at the CERN SPS muon beam with a high-luminosity spectrometer which is shown in Fig.1 and is described in more detail elsewhere[1]. It consists of a 40 m long segmented toroidal iron magnet which is magnetized close to saturation and surrounds a 30 m long "internal" liquid hydrogen target. The iron absorbs the hadronic shower after a few meters and the surviving scattered muon is focused towards the spectrometer axis. The toroids are instrumented with scintillation trigger counters and multiwire proportional chambers. A 10 m long "external" target in front of the spectrometer magnet extends the acceptance of the apparatus to smaller angles, i.e. to smaller values of x and Q^2, than are accessible with the targets inside the iron. Four hodoscopes along the spectrometer axis detect the incoming muons and measure their trajectories. The momentum of the incident muons is measured with a spectrometer consisting of an air-gap magnet and another four scintillator hodoscopes upstream of the apparatus. Results from a similar measurement with a carbon target have been presented earlier[2,3].

The analysis presented here is based on $2\cdot10^6$ reconstructed events after all cuts recorded with positive muon beams of 100, 120, 200 and 280 GeV energy. The kinematic ranges and data samples are summarized in Table 1. The principle sources of systematic errors in the data are uncertainties in:

the calibration of the incident beam energy ($\Delta E/E < 1.5 \cdot 10^{-3}$),
the calibration of the spectrometer magnetic field ($\Delta B/B < 2 \cdot 10^{-3}$),
the corrections for the energy loss of muons in iron[4],
the corrections for the finite resolution of the spectrometer ($\Delta\sigma/\sigma < 5 \cdot 10^{-2}$),
the relative luminosity calibration (normalization) between data taken at different beam energies (1%),
the absolute cross section normalization (3%).

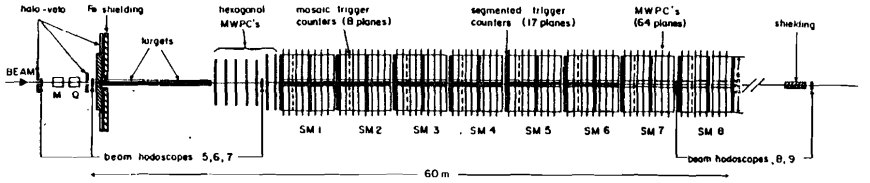

Fig.1. Schematic view of the apparatus.

Most of the results presented in this paper, especially those on R and on the comparison of scaling violations to QCD predictions, are affected by the uncertainty on the relative but not the absolute cross section normalization. A more detailed discussion of the treatment of the systematic errors and of the calibrations undertaken to minimize them can be found in ref.[2].

The data analysis is similar to the one described in ref.[2]. The only difference is due to the additional external targets which were installed after completion of the carbon target experiment. For events originating from the internal targets, the geometrical acceptance is greater than 65% and is rather flat in the kinematic region $x > 0.25$ and $Q^2/2ME > 0.15$ where M is the proton mass. For events from the external targets, the acceptance depends on the beam energy and on the position of the interaction vertex along the beam direction. Structure functions were therefore evaluated separately for the two target regions. The background from target wall interactions was determined from special empty target runs and was subtracted from the data. At all beam energies, the data from external and internal targets were found to be in statistical agreement and were combined for the subcequent analysis. Radiative corrections were applied using the

calculations of refs.[5]. The error on $F_2(x,Q^2)$ from uncertainties on these corrections is estimated to be smaller than 1%.

$R = \sigma_L/\sigma_T$ was determined by comparing the F_2 measurements at different beam energies. F_2 was first evaluated under the assumption that R equals zero. R was then varied, and therefore $F_2(x,Q^2)$ varied simultaneously according to eq. (1), such that the χ^2 of the four data sets with respect to a common phenomenological parametrization of the Q^2 dependence of F_2 is minimized. This was done separately in each bin of x under the assumption that R is independent of Q^2, consistent with QCD calculations which predict only a weak (logarithmic) variation of R with Q^2 [6]

$$R_{QCD}(x,Q^2) = \frac{F_L(x,Q^2)}{(1+4M^2x^2/Q^2)\cdot F_2(x,Q^2) - F_L(x,Q^2)}, \qquad (2)$$

where

$$F_L(x,Q^2) = \alpha_s(Q^2)/2\pi \cdot x^2 \cdot \int_x^1 \left[\frac{8}{3}F_2(z,Q^2) + \frac{40}{9}\left(1-\frac{x}{z}\right) z G(z,Q^2)\right] dz/z^3 \qquad (3)$$

is the longitudinal structure function and $\alpha_s(Q^2)$ is the running coupling constant of QCD. R_{QCD} is computed assuming a gluon momentum distribution $xG(x,Q^2) = 5.5 \cdot (1-x)^{10}$ at $Q_0^2 = 5\ GeV^2$ and a QCD mass scale parameter $\Lambda = 210$ MeV. Equation (3) does not account for effects of the charm quark mass which were included following ref.[7]. The measurement of R and the QCD prediction are shown in Fig.2 together with earlier EMC data[8] from a hydrogen target. At $x > 0.25$, the measured values are small and are compatible with zero in agreement with our carbon target measurement[2]. At small x, the data show a rise compatible with the QCD prediction.

R_{QCD} was used to compute the final structure functions at the four different beam energies (Fig.3). The excellent agreement between the different data sets in the region of large x constitutes a powerful cross-check of the spectrometer calibrations as is discussed in more detail in ref.[2]. The final $F_2(x,Q^2)$ from the combined data sets is shown in Fig.4 together with the EMC data[8] and with the SLAC-MIT results from electron-proton scaling at low Q^2 [9]. The agreement with the EMC data is poor especially at small x where the F_2 measured in this experiment is larger by up to 20%. A similar trend was observed in our measurement on a carbon target[2] which indicated a steeper x dependence of F_2 than measured in earlier experiments. A direct comparison to the SLAC data is more difficult since the experiments cover disjoint ranges of Q^2.

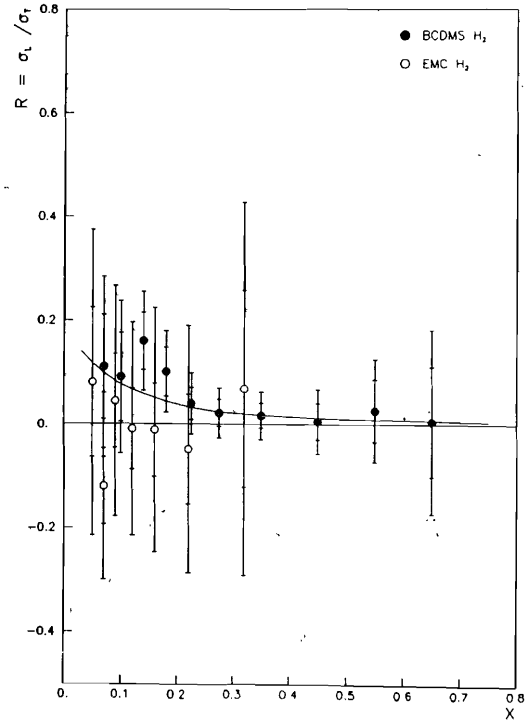

Fig.2. $R = \sigma_L / \sigma_T$ as a function of x. Also shown is the measurement by the EMC collaboration on a hydrogen target[8]. Inner error bars are statistical only, outer error bars are statistical and systematic errors combined linearly. The solid line is the QCD prediction for α_s in next-to-leading order, $\Lambda_{\overline{MS}} = 210$ MeV, and a gluon distribution $xG(x) = 5.5(1-x)^{10}$ at $Q_o^2 = 5$ GeV^2.

The data exhibit clear deviations from Bjorken scaling. In the framework of perturbative QCD[10], scaling violations are due to the Q^2 evolution of quark and gluon distribution which can be described by the Altarelli-Parisi equations[11] or can alternatively be expressed through the Q^2 dependence of their moments[12]. Higher twist contributions to F_2 from quark-quark interactions which are not described by the QCD evolution equations are expected to vary like power series in $1/Q^2$ [18] and are therefore unimportant over most of the Q^2 range of the data. Furthermore, the data extend up to $x = 0.75$, thus requiring only little extrapolation to calculate the evolution integrals. Our measurement is therefore well suited for a precise test of the evolution equations.

Several numerical methods have been developed to fit the predictions of the evolution equations to the experimental data. We have mainly employed two methods[14,13] which have been developed within our collaboration. They allow to fit the flavour singlet and nonsinglet evolution equations both in a leading order (LO) perturbation ex-

pantion and in a next-to-leading order expansion in the $\overline{MS}$ renormalization scheme. A short description of these programs can be found in ref.[3].

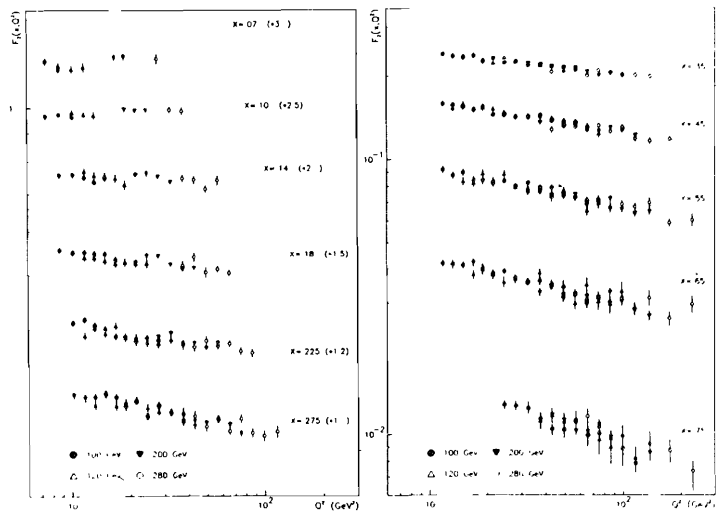

Fig.3. The proton structure function $F_2(x,Q^2)$ for $R = R_{QCD}$ measured at the four beam energies 100, 120, 200 and 280 GeV. Only statistical errors are shown.

The experimental data shown in Fig.3 were used for the fits, excluding points with $y < 0.2$ to reduce the sensitivity to spectrometer calibration uncertainties. The QCD analysis was performed both in a nonsinglet approximation and in a complete singlet and nonsinglet treatment. The region of $x \geq 0.275$ was used in the nonsinglet approximation where the gluon distribution is ignored. This is justified by estimates of the gluon distribution from earlier muon[3,8,15] and neutrino scattering experiments[16,17]. Data points at $Q^2 < 20$ GeV^2 were excluded to further reduce the contribution of the gluon distribution which becomes softer with increasing Q^2 due to its QCD evolution. The results of these fits are summarized in Table 2. We find good agreement between the values of Λ obtained with the different programs and statistical agreement with fits to our carbon target data covering a very similar kinematic range [3]. Our best estimate for the QCD mass scale parameter at next-to-leading order is

$$\Lambda_{\overline{MS}} = 210 \pm 20 \text{ (stat.) MeV},$$

corresponding to a strong coupling constant of

$$\alpha_s = 0.157 \pm 0.003 \text{ (stat.)}$$

at $Q^2 = 100\ \text{GeV}^2$.

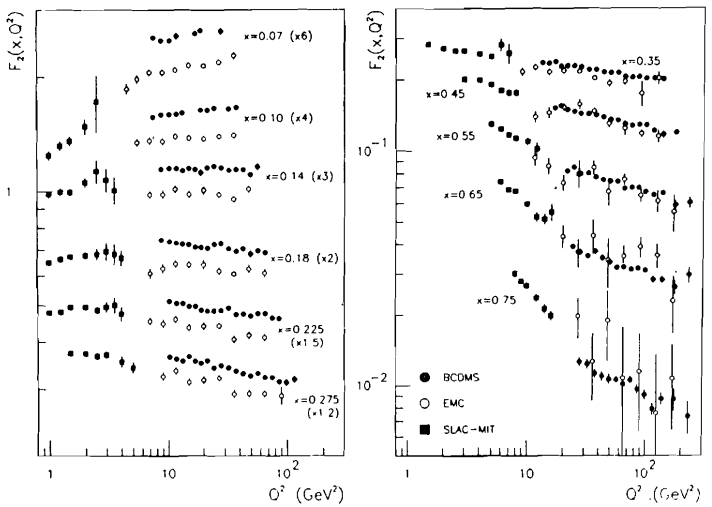

Fig.4. The structure function $F_2(x,Q^2)$ using $R = R_{QCD}$ for all beam energies combined, compared to the data from the EMC[8] and SLAC-MIT[9] experiments. The SLAC-MIT and EMC data are rebinned to the x values of this experiment; note that there are no SLAC data in the lowest x bin. The relative normalization between the experiments has not been adjusted. Only statistical errors are shown.

The detailed evaluation of the systematic error on Λ has not yet been completed, but it is expected to be similar to that of our carbon target measurement ($\Delta\Lambda$ = 60 MeV (syst.)) [2,3]. This systematic error is mainly due to the relative normalization uncertainties between the measurements at different beam energies. Since these are uncorrelated between the carbon and hydrogen target experiments, the good agreement between the two indicates that the systematic error may be overestimated.

Conventionally, Λ has been determined from global QCD fits to $F_2(x,Q^2)$ which do not, however, constitute a sensitive test of Quantum Chromodynamics. The χ^2 s of such fits describe mainly their agreement with the x dependence of F_2 which is not predicted by the theory. A more stringent test is obtained by comparing the x dependence of the scaling violations observed in the data to the one expected from the QCD evolution. This is the only specific prediction of perturbative QCD for deep inelastic scattering which can be tested experimentally. In the nonsinglet approximation, this comparison depends on Λ as the only free parameter whereas over the full x range it is also sensitive to the gluon distribution. The nonsinglet case is shown in Fig. 5a where the logarithmic derivatives $d\ln F_2(x,Q^2)/d\ln Q^2$ are compared to the next-to-leading order prediction for $\Lambda_{\overline{MS}}$ = 210 MeV.

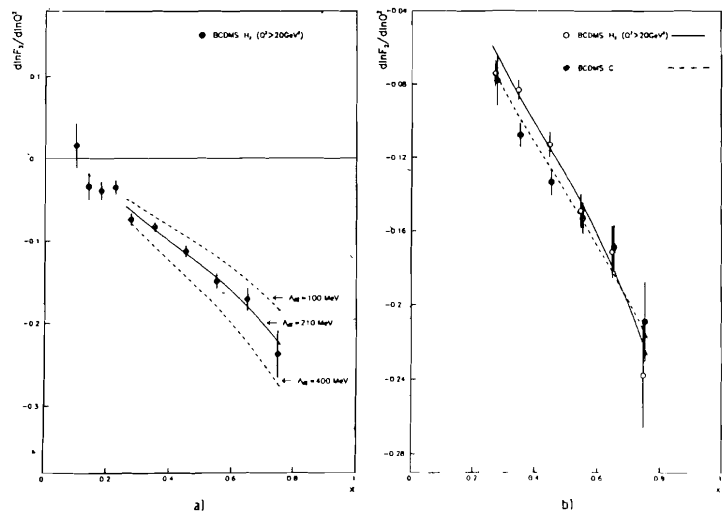

Fig.5. (a) Scaling violations observed in this experiment at $Q^2 > 20\ \text{GeV}^2$ expressed as logarithmic derivatives $d\ln F_2(x,Q^2)/d\ln Q^2$, as a function of x. The errors are statistical only. The lines show nonsinglet QCD predictions for $\Lambda_{\overline{MS}}$ = 210 MeV corresponding to our fit with the method of [13] (χ^2/DOF=3.8/5), and for two other values of Λ.
(b) As (a), compared to carbon target results from the same experiment[3].

The logarithmic derivatives in Fig. 5a are the slope parameters of straight line fits $\ln F_2 = a \cdot \ln Q^2 + b$ to the data. To calculate the theoretical predictions shown in the same figure, the results of the QCD fit F_2' were assigned at each (x,Q^2) point the statistical er-

ror of the corresponding experimental F_2. The logarithmic derivatives $d\ln F_2'/d\ln Q^2$ were then obtained by the same straight line fit as for the experimental data. Within the errors, this linear representation is an excellent approximation of both the experimental and the predicted Q^2 evolution. The measured x dependence of the scaling violations in Fig. 5a is in agreement with the predicted one within statistical errors ($x^2/DOF = 3.8/5$). In Fig. 5b, the scaling violations are compared to the measurement of ref./3/. The data show a difference between proton and carbon target which is consistent with the QCD prediction and is due to the steeper x dependence of F_2 measured on an isoscalar target.

Table 1: The data sample

Beam energy (GeV)	Q^2 range (GeV^2)	x range	Number of events
100	7- 80	0.06-0.8	570 000
120	8-106	0.06-0.8	420 000
200	16-150	0.06-0.8	800 000
280	26-260	0.06-0.8	190 000

Table 2: Results of nonsinglet QCD fits to $F_2(x,Q^2)$ at $x \geq 0.275$ and $Q^2 \geq 20$ GeV^2

	Λ_{LO} (MeV)	χ^2/DOF	$\Lambda_{\overline{MS}}$ (MeV)	χ^2/DOF
Ref. [13]	182±20	169/180	211±22	169/180
Ref. [14]	184±20	170/180	201±20	168/180
Carbon target [3]	210±20		230±20	

Table 3: Results of singlet+nonsinglet QCD fits to $F_2(x,Q^2)$ at $x \geq 0.07$ and $Q^2 \geq 10$ GeV^2

Method	Λ_{LO} (MeV)	η_{LO}	χ^2/DOF	$\Lambda_{\overline{MS}}$ (MeV)	$\eta_{\overline{MS}}$	χ^2/DOF
Ref. [13]	196±19	5.2±1.5	281/282	214±19	10.3±1.5	282/282
Ref. [14]	183±25	5.4±1.3	269/277	195±20	8.9±1.5	270/277

For the QCD analysis over the full x range of the data, the proton structure function is decomposed into a singlet (S) and a nonsinglet(NS) part as/10/

$$F_2(x,Q^2) = {}^5/_{18} F_2^S(x,Q^2) + {}^1/_6 F_2^{NS}(x,Q^2), \quad (4)$$

where F_2^{NS} and F_2^S follow different Q^2 evolutions. All data points at $Q^2 > 10$ GeV^2 are used in these fits. The gluon momentum distribution is parametrized as $xG(x,Q^2) = A(\eta + 1)(1-x)^\eta$ at $Q_o^2 = 5$ GeV^2 and is allowed to evolve with Q^2. From the energy-momentum sum rule, A equals the fraction of the total proton momentum carried by gluons and is found to be $A = 0.45$ at $Q^2 = 5$ GeV^2.

We have adopted two different approaches to determine the parameter η from the measured scaling violations. In the first method, the program of ref./13/ was used and the nonsinglet part of F_2 ($F_2^{NS} = (u + \bar{u} - d - \bar{d})$) was constrained experimentally using preliminary results on the deuterium structure function from our experi-

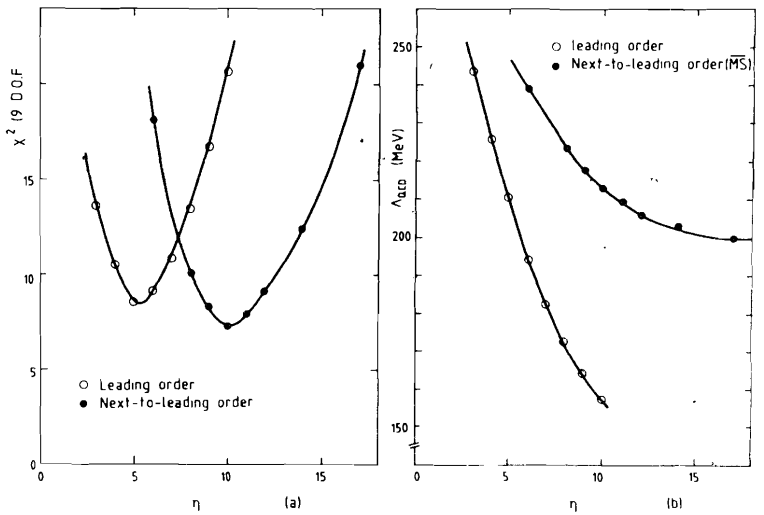

Fig.6. (a) The χ^2 of the comparison of measured and predicted scaling violations as a function of η for leading and next-to-leading order fits.
(b) The QCD mass scale Λ as a function of the power η of a gluon distribution $xG(x,Q_o^2) = A(\eta + 1)(1-x)^\eta$ at $Q_o^2 = 5$ GeV^2 from flavour singlet+nonsinglet fits at leading and next-to-leading order.

ment[19]. The effect of the charm threshold is small but was taken into account using the method of ref.[7]. Λ was fitted together with parametrization of the singlet part of F_2 for fixed values of η. For each value of η the χ^2 of the comparison of measured and fitted scaling violations was determined in the same way as for the nonsinglet fits discussed above. These χ^2's are shown in Fig. 6a and exhibit different minima for the leading and next-to-leading order fits. Λ and η corresponding to these minima are shown in Table 3. The results for Λ are in good agreement with those of the nonsinglet fits. The correlation between η and Λ is shown in Fig. 6b. In next-to-leading order, we find a very soft gluon distribution which explains the weak dependence of $\Lambda_{\overline{MS}}$ on η and justifies a posteriori the nonsinglet fits of $\Lambda_{\overline{MS}}$ discussed above. The measured scaling violations are compared in Fig. 7 to next-to-leading order fits for different values of η and show again very good agreement with the theoretical prediction.

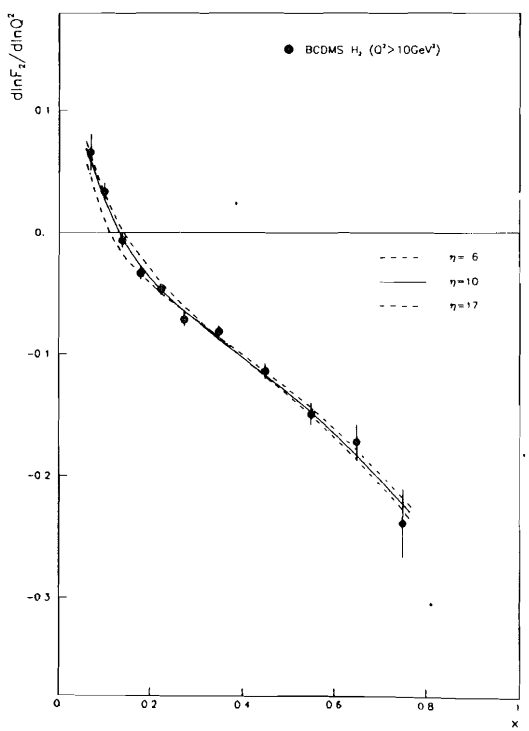

Fig.7. Scaling violations observed in this experiment at $Q^2>10GeV^2$, expressed as logarithmic derivatives $d\ln F_2(x,Q^2)/d\ln Q^2$. The errors are statistical only. Also shown are combined singlet+nonsinglet predictions in next-to-leading order QCD for different powers η of a gluon distribution parametrized as $xG(x,Q^2)=A(\eta+1)(1-x)^\eta$ at $Q_0^2=5GeV^2$. The fits with η=6,10 and 17 yield $\Lambda_{\overline{MS}}$ = 239,213 and 200 MeV, respectively.

For the second method, we use the program of ref.[14]. The singlet and nonsinglet parts of F_2 are parametrized separately and fitted to the data together with Λ and η. The results are also given in Table 3 and are in good agreement with the first method.

The gluon distributions in leading and next-to-leading order are shown in Fig. 8 together with the earlier leading order EMC result from proton target data[8]. They are valid only in the range $0.06 \leq x \leq 0.30$ since there are no F_2 data at smaller x and at large x the fit becomes insensitive to the exponent η of the parametrization.

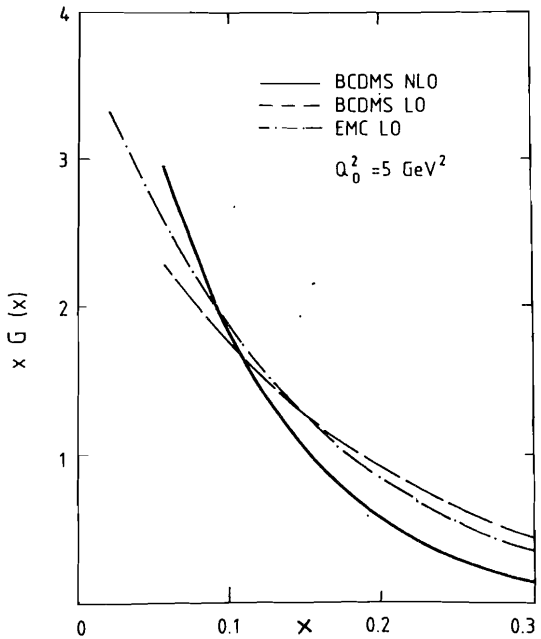

Fig.8. The gluon momentum distribution in the proton determined in leading and next-to-leading order QCD from this experiment, compared to the earlier leading order analysis from the EMC /8/ experiment. No statistical or systematic errors are shown.

In conclusion, we have presented a new high statistics measurement of the proton structure function $F_2(x,Q^2)$ from deep inelastic muon scattering at high Q^2 on a hydrogen target. $R = \sigma_L/\sigma_T$ determined from these data is in good agreement with predictions from perturbative QCD. From flavour nonsinglet and from combined singlet and nonsinglet fits, we find a QCD mass scale parameter $\Lambda_{\overline{MS}} = 210 \pm 20$ MeV. The scaling violations observed in the data are in quantitative agreement with QCD predictions, showing that this determination of Λ is based on an excellent overall description of the data by the theory. The gluon distribution has been determined for the first time from singlet fits in next-to-leading order QCD and is found to be significantly softer than in leading order.

References

1. BCDMS, D. Bollini et al., Nucl.Instr.Meth. 204 (1983) 333;
   BCDMS, A.C. Benvenuti et al., Nucl.Instr.Meth. 226(1984)330.
2. BCDMS, A.C. Benvenuti et al., CERN-EP/87-100.
3. BCDMS, A.C. Benvenuti et al., CERN-EP/87-101.
4. BCDMS, R. Kopp et al., Z.Phys. C28(1985) 171;
   W. Lohmann, R. Kopp and R. Voss, CERN 85-03 (CERN Yellow Report).
5. A.A. Akhundov et al., Sov.J.Nucl.Phys.26(1977) 660;
   D.Yu. Bardin and N.M. Shumeiko, Sov.J.Nucl.Phys. 29(1979) 499;
   A.A. Akhundov et al., Yad.Fiz. 44(1986) 1517;
   A.A. Akhundov et al., Preprint JINR E2-86404, Dubna, 1986.
6. G. Altarelli and G. Martinelli, Phys.Lett 76B(1978) 89.
7. M. Glück, E. Hoffmann and E. Reya, Z.Phys. 13(1982) 119.
8. EMC, J.J. Aubert et al., Nucl.Phys. B259(1985) 189.
9. A. Bodek et al., Phys.Rev. D20 (1979) 1471.
10. For an extensive review of perturbative QCD and further references, see G. Altarelli. Phys.Rep.81(1982)1.
11. G. Altarelli and G.Parisi, Nucl.Phys. B126(1977) 298.
12. For a review, see D.W. Duke and R.G. Roberts, Phys.Rep 120(1985) 275.
13. M. Virchaux and A. Ouraou, Preprint DPhPE 87-15, to be published.
14. V.G. Krivokhizhin et al., Preprint JINR E2-86-564.
15. EMC, J.-J. Aubert et al., Nucl.Phys. B272 (1986) 158.
16. CDHS, H. Abramowicz et al., Z.Phys. C17(1983) 283.
17. CHARM, F. Bergsma et al., Phys.Lett. 123B(1983) 269.
18. R.K. Ellis et al., Nucl.Phys. B212 (1983) 29;
    J.C. Corton and J. Sanchez Guillen, Phys.Lett. 120B(1983)29.
19. BCDMS, A.C. Benvenuti et al., to be published.

Бенвенути А. и др. E1-87-689

Измерение структурной функции протона с высокой статистической точностью и проверка КХД с помощью глубоконеупругого рассеяния мюонов при больших Q^2

Приведены предварительные результаты измерения структурных функций протона $F_2(x,Q^2)$, а также $R = \sigma_L/\sigma_T$. Результаты получены в опытах по глубоконеупругому рассеянию мюонов на водороде на большом статистическом материале. Для анализа данных было отобранно $2\cdot10^6$ событий, зарегистрированных при энергиях 100, 120, 200 и 280 ГэВ, которые принадлежат кинематической области $0,06 \le x \le 0,80$ и $7\ \text{ГэВ}^2 \le Q^2 \le 260\ \text{ГэВ}^2$. Выполнено сравнение наблюдаемых нарушений скейлинга с предсказаниями теории КХД, в ходе которого оказалось возможным определить масштабный пераметр КХД Λ и оценить распределение глюонов в протоне.

Препринт Объединенного института ядерных исследований. Дубна 1987

Benvenuti A.C. et al E1-87-689

A High Statistics Measurement of the Proton Structure Function and Tests of QCD from Deep Inelastic Muon Scattering at High Q^2

We present preliminary results on a high statistics measurement of the proton structure functions $F_2(x,Q^2)$ and $R = \sigma_L/\sigma_T$ measured in deep inelastic scattering of muons on hydrogen. The analysis is based on $2\cdot10^6$ events after all cuts recorded at beam energies of 100, 120, 200 and 280 GeV and covering a kinematic range $0.06 \le x \le 0.80$ and $7\ \text{GeV}^2 \le Q^2 \le 260\ \text{GeV}^2$. Scaling violations which are observed in the data are compared to predictions of perturbative QCD. They allow to determine the QCD mass scale parameter Λ and to estimate the distribution of gluons in the proton.

Preprint of the Joint Institute for Nuclear Research. Dubna 1987